2024 International Nuclear Atlantic Conference – INAC 2024

Escola de Guerra Naval, Rio de Janeiro, RJ, May 6 - 10, 2024

ISBN: 978-65-594-1256-3

Thermal evaluation of a Cs-loaded waste vitrification

Costa-Silva, D.L.[1]; Araujo, M.S.[1];
Fungaro, D.A.[2]; Mello-Castanho. S.R.[1]

[1] *danilo.silva@ipen.br, Correspondence Address*

[1]Centro de Ciência e Tecnologia de Materiais – CECTM – Instituto de Pesquisas Energéticas e Nucleares (IPEN/USP)
[2]Centro de Química e Meio Ambiente – CEQMA – Instituto de Pesquisas Energéticas e Nucleares (IPEN/USP)

1. Introduction

The vitrification of high-level waste (HLW) is the most broadly process used for the treatment of wastes generated from the reprocessing of spent nuclear fuel[1]. Many glass compositions have been developed for more than 50 year, and borosilicate glass compositions are definitely a good choice for this application, basically due to their good thermal shock resistance and excellent accommodation of most of the radionuclides that are found in the radioactive wastes[2]. Today, the HLW melters facilities are performed by two processes: the Atelier de Vitrification de La Hague (AVH) and the liquid-fed joule-heated ceramic-lined melter (LFCM)[3]. However, besides the problems related to the vitrification process such as undesired phase crystallization[4] in the melters for sodium and aluminun-rich HLW, there are also problems related to the radiation-induced heating such as devitrification, and structural defects such as bubbles, volume changes and the transmutation of radionuclides[4–8]. Among the extended list of radionuclides present in inventories[2], ^{137}Cs is one of the most dangerous due to its half-live of 30,2 years, high activity (10^{15} Bq) and ease of contamination through soil and rivers[9].

This work evaluates the thermal effects of the vitrification of a Cs-loaded zeolite (simulated ^{137}Cs-rich waste) by using a glass composition of the soda-lime silicate family doped with B and Nb. Changes in the thermal properties of the matrix after the incorporation of the simulated Cs waste showed that the referred glass matrix is an adequate composition towards obtaining wasteforms with improved thermal stability for radiation-induced heating and devitrification (around 520 °C), which is a promising characteristic for its use in the selective vitrification of all Cs radionuclides (^{134}Cs, ^{135}Cs and ^{137}Cs).

2. Methodology

The glass matrix (G3) was produced according to the procedure found in our previous work[10] and the nominal composition is shown in Table 1.

Table 1 – Nominal composition of the glass matrix G3[10].

Oxide	SiO_2	B_2O_3	Na_2O	CaO	K_2O	Al_2O_3	Nb_2O_5
wt.%	40.68	7.96	25.37	19.80	0.99	1.99	3.21

The glass precursors were homogenized and transferred to an alumina crucible for the melting at 1300 °C for 2h in an electrical furnace, followed by casting onto metallic plate for super-fast cooling and solidification. To produce the vitrified Cs waste, glass precursors were mixed with Cs-loaded zeolite A (3:2), and the same stages as the procedure for glass wasteform synthesis were repeated. Differential Thermal Analysis (DTA) of

the glass samples was performed on a Netzsch DSC/DTA 404F3 equipment, in synthetic air, at 10ºC/min. up to 1300ºC.

3. Results and Discussion

The thermograms of the glass samples before and after the incorporation of the Cs-loaded waste is shown in Figure 1. The first exothermic deviation is the glass transition (T_g) and represents the loosening of the network structure. The T_g changes from 500 °C (G3) to 523 °C (G3 + Cs-loaded waste), suggesting that the vitrified waste glass exhibits an increase in the strength of the network structure, when compared to G3, as observed by Bouras et al.[11] The second thermal event is the exothermic peak, due to the complete devitrification of the glasses. Such event varies from 700 °C (G3) to around 828 °C (G3 + Cs-loaded waste), and the increase in the interval from T_g to the initial devitrification suggests that the sample G3 + Cs-loaded waste is thermally more stable than G3[12]. Then the third important event is endothermic and represents the melting of the crystals that were grown in the devitrification process. This melting occurred at 950 °C for G3 and 980 °C for the vitrified waste glass (G3 + Cs-loaded waste), and such change is also a consequence of the compositional increment[11].

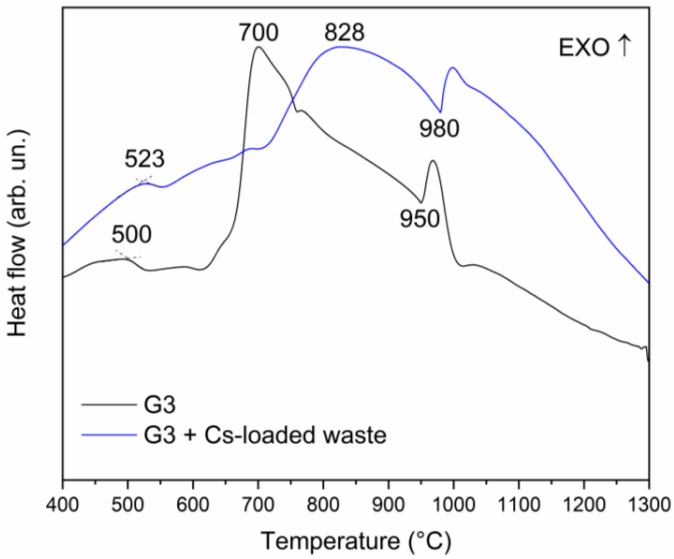

Figure 1: Differential thermal analysis (DTA) of the glass matrix before (G3) and after (G3 + Cs-loaded waste) the incorporation of 40 wt.% of the simulated Cs waste.

The differences in the thermal behavior were assessed by plotting the composition of four sub-systems in ternary phase diagrams: SiO_2:Na_2O:CaO, SiO_2:Al_2O_3:Na_2O, Na_2O:B_2O_3:Nb_2O_5 and SiO_2:Al_2O_3:Cs_2O before and after the Cs-loaded waste incorporation, the results are respectively shown in Figure 2 (a -d), and the compositions of the referred sub-systems are shown in Table 2. It is observed (Figure 2 a and b) that for the sub-systems SiO_2:Na_2O:CaO and SiO_2:Al_2O_3:Na_2O, the vitrification of the Cs-loaded waste in the G3 glass matrix projects the composition to a different compatibility triangle, and this results in increased liquidus temperatures and different proportions of the crystallized phases. For the case of the sub-system Na_2O:B_2O_3:Nb_2O_5 (Figure 2-c), it is observed that the vitrification of the Cs-loaded waste projects the composition to higher liquidus temperatures (1300 °C) than for G3 glass matrix (1200 °C), and both are in the $NaNbO_3$ crystallization field. Considering the SiO_2:Al_2O_3:Cs_2O system (Figure 2-d), it is observed that the plotted composition lies in the Pollucite ($CsAlSi_2O_6$) crystallization field. In this case, Cs atoms that act as modifier cations might compete with Na for charge stabilization on the SiO_4^- and AlO_4^- units[10].

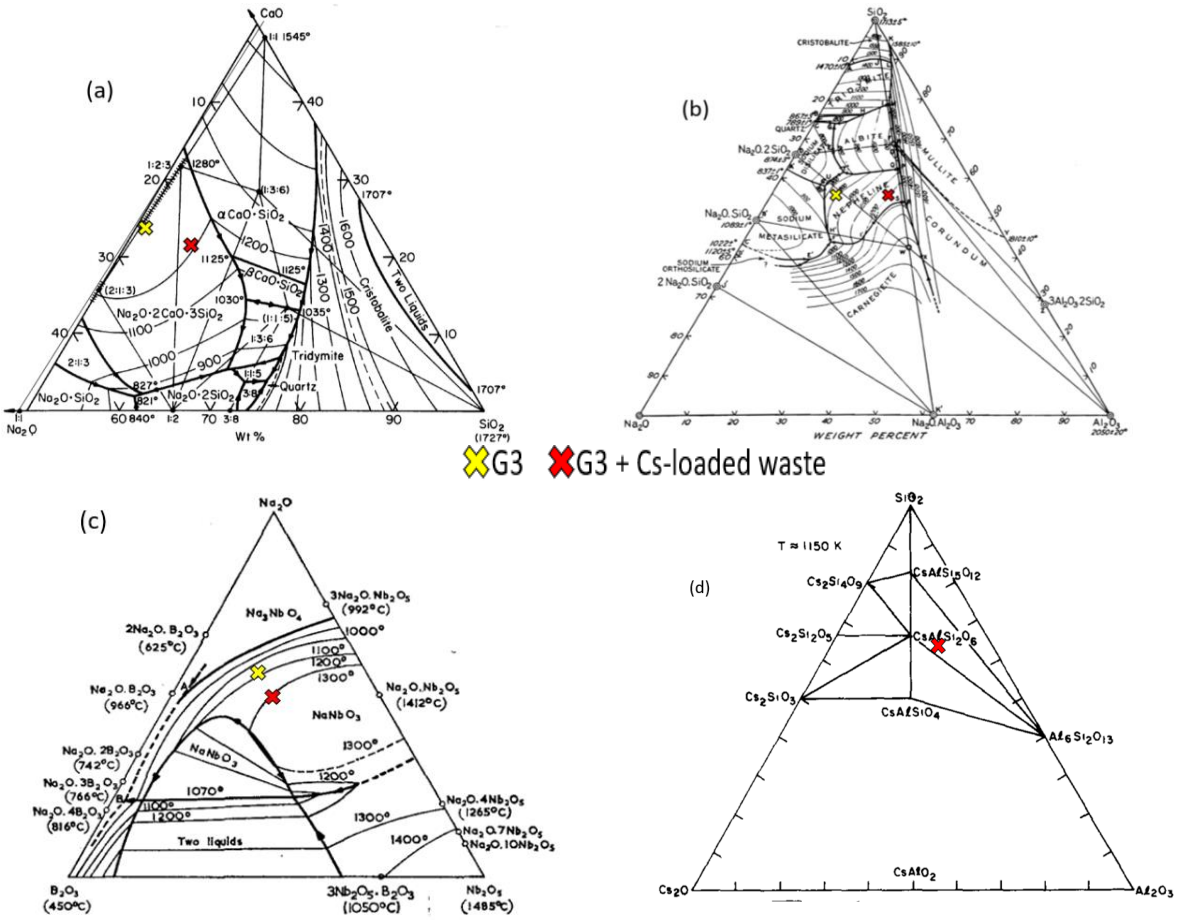

Figure 2: Ternary equilibrium phase diagrams of the sub-systems: (a) SiO_2:Na_2O:CaO, (b) SiO_2:Al_2O_3:Na_2O, (c) Na_2O:B_2O_3:Nb_2O_5 and (d) SiO_2:Al_2O:Cs_2O[13]

Table 2: Concentration (wt.%) of compounds in the sub-systems before and after the vitrification of the Cs-loaded waste.

Sub-systems	(a)			(b)			(c)			(d)		
Oxide	SiO_2	Na_2O	CaO	SiO_2	Na_2O	Al_2O_3	B_2O_3	Na_2O	Nb_2O_5	SiO_2	Al_2O_3	Cs_2O
G3	48.6	26.2	25.2	56.5	30.5	13.0	22.5	55.2	22.3	-	-	-
G3 + Cs-loaded waste	57.6	20.5	20.5	57.6	20.5	21.9	18.5	51.2	30.4	64.9	24.7	10.4

4. Conclusions

The selective vitrification of Cs radionuclides was thermally studied by incorporating Cs-loaded waste into a soda-lime silicate glass matrix doped with B and Nb. The waste glass (G3 + Cs-loaded waste) is adequate for the immobilization of HLW due to its improved thermal stability, which was a result of the compositional increment related to the simulated waste, as the ternary phase diagrams projected the vitrified compositions in different compatibility triangles and liquidus temperatures. The Cs atoms are likely to compose pollucite crystals under devitrification. Future works can be performed by increasing the waste loading and studying its influence on the structure and homogeneity.

Acknowledgements

This work was supported by the Instituto de Pesquisas Energéticas e Nucleares (IPEN) with laboratory facilities and post-doctoral scholarship by project n°2018.05.IPEN.14.

References

[1] A. Sakai, S. Ishida, "Reflective reviews on Japanes high-level waste (HLW) vitrification – Exploring the obstacles encountered in active tests at Rokkasho", *Ann. Nucl. Energy,* vol. 196, pp. 110175 (2024).

[2] S. Caruso, A. Meleshyn, U. Noseck, "Estimation and comparison of the radionuclide inventories in vitrified high-level wastes from reprocessing plant", *Progress in Nucl. Energy,* vol. 94, pp. 216-221 (2017).

[3] C.M. Jantzen, in *Handbook of Advanced Radioactive Waste Conditioning Technologies,* Woodhead, Cambridge-UK (2011).

[1] A. Sakai, and S. Ishida, "Reflective reviews on Japanese high-level waste (HLW) vitrification – Exploring the obstacles encountered in active tests at Rokkasho," *Ann Nucl Energy,* vol. 196, pp. 110175 (2024).

[2] S. Caruso, A. Meleshyn, and U. Noseck, "Estimation and comparison of the radionuclide inventories in vitrified high-level wastes from reprocessing plant," *Progress in Nuclear Energy,* vol. 94, (2017).

[3] C.M. Jantzen, in *Handbook of Advanced Radioactive Waste Conditioning Technologies,* Woodhead, Cambridge-UK (2011).

[4] A. Goel, J.S. McCloy, R. Pokorny, and A.A. Kruger, "Challenges with vitrification of Hanford High-Level Waste (HLW) to borosilicate glass – An overview," *Journal of Non-Crystalline Solids: X,* vol. 4, pp. 100033 (2019).

[5] P. Rautiyal, G. Gupta, R. Edge, L. Leay, A. Daubney, M.K. Patel, A.H. Jones, and P.A. Bingham, "Gamma irradiation-induced defects in borosilicate glasses for high-level radioactive waste immobilisation," *Journal of Nuclear Materials***,** vol. 544, pp. 152702 (2021).

[6] W.J. Weber, "Radiation and Thermal Ageing of Nuclear Waste Glass," *Procedia Materials Science***,** vol. 7, pp. 237–246 (2014).

[7] W.J. Weber, and F.P. Roberts, "A review of radiation effects in solid nuclear wast forms," *Nucl Technol, vol.* 60 (2), pp. 178-198 (1983).

[8] R.C. Ewing, W.J. Weber, and F.W. Clinard, "Radiation effects in nuclear waste forms for high-level radioactive waste," *Progress in Nuclear Energy,* vol. 29 (2), pp. 63–127 (1995).

[9] A. V. Voronina, A.Y. Noskova, V.S. Semenishchev, and D.K. Gupta, "Decontamination of seawater from 137Cs and 90Sr radionuclides using inorganic sorbents," *J Environ Radioact,* vol. 217, pp. 106210 (2020).

[10] D.L. Costa-silva, J.F. Bartolomé, A.C. Silva, and S. Mello-Castanho, "Structural and thermal influence of niobia in aluminoborosilicate glasses," *Ceram Int***,** vol. 48 (13), pp. 18433–18440 (2022).

[11] N. Bouras, M.A. Madjoubi, M. Kolli, S. Benterki, and M. Hamidouche, “Thermal and mechanical characterization of borosilicate glass,” *Phys Procedia*, vol. 2 (3), pp. 1135–1140 (2009).

[12] Swapna, G. Upender, and M. Prasad, “Raman, FTIR, thermal and optical properties of TeO_2-Nb_2O_5-B_2O_3-V_2O_5 quaternary glass system,” *Journal of Taibah University for Science*, vol. 11 (4), pp. 583-592 (2017).

[13] Robert S. Roth, Taki Negas, and Lawrence P. Cook, *Phase Diagrams for Ceramists*, American Ceramic Society, Michigan – USA, 1981.